Available online at www.sciencedirect.com
ScienceDirect
Nuclear Physics B Proceedings Supplement 00 (2012) 1–5
Nuclear Physics B Proceedings Supplement

Studies of $B \to \tau\nu$ and $B \to D^{(*)}\tau\nu$ decays at *BABAR*

Georges Vasseur

CEA, IRFU, SPP, Centre de Saclay, F-91191 Gif sur Yvette, France

Abstract

Decays of B mesons into final states containing a τ lepton are sensitive to new-physics contributions involving charged Higgs bosons or other charged-current interactions that violate lepton universality. The *BABAR* experiment has reported evidence for the decay $B \to \tau\nu$ and observed significant signals for the decays $B \to D^*\tau\nu$ and $B \to D\tau\nu$. The agreement of these results with the Standard-Model expectation is evaluated, and tight constraints are placed on type-II two-Higgs-doublet-model scenarios.

Keywords: Bottom mesons, Leptonic and semileptonic decays, Supersymmetric Higgs bosons

1. Introduction

The recent analyses of $B \to \tau\nu$ leptonic decays [1] and $B \to D^{(*)}\tau\nu$ semileptonic decays [2] performed by the *BABAR* collaboration allow to test the predictions from the Standard Model (SM) and search for new-physics effects, such as charged-current interactions that violate lepton universality. In particular the $B \to \tau\nu$ and $B \to D^{(*)}\tau\nu$ decays are sensitive to the presence of a charged Higgs boson.

The *BABAR* detector [3] was installed on the PEP-II energy asymmetric e^+e^- collider at SLAC. Charges particles are reconstructed in a silicon vertex tracker and a drift chamber, and identified with a DIRC Cerenkov detector. Photons and electrons are measured in a CsI electromagnetic calorimeter. All these detectors are inside a solenoid creating a 1.5 T magnetic field. Muons are detected in muon chambers located in the flux return of the solenoid. *BABAR* took data from 1999 to 2008. The final dataset, which is used in the analyses presented here, consists of 470 millions of $B\bar{B}$ pairs.

In the $B \to \tau\nu$ and $B \to D^{(*)}\tau\nu$ analyses, there are two or three neutrinos in the final state, hence a lot of missing momentum and a lack of kinematics constraints for the signal. In order to reduce the huge background, the following technique is used in both analyses. An exclusive decay of one of the two B mesons in the event, referred as tag-B, is first reconstructed fully in various hadronic modes. The rest of the event is then examined for the signal searched for.

2. $B \to \tau\nu$ decays

The purely leptonic $B^+ \to \ell^+\nu_\ell$ decays are of particular interest to test the SM as the prediction of their branching ratio in the SM is very clean theoretically:

$$\mathcal{B}_{SM}(B^+ \to \ell^+\nu_\ell) = \frac{G_F^2\, m_B\, m_\ell^2}{8\pi}\left[1 - \frac{m_\ell^2}{m_B^2}\right]^2 f_B^2\, |V_{ub}|^2\, \tau_B.$$

G_F is the Fermi constant, m_B the B-meson mass, and τ_B the B-meson lifetime. The main uncertainties on this prediction come from the B meson decay constant f_B and the CKM matrix element $|V_{ub}|$. As the branching ratio is proportional to the square of the lepton mass m_ℓ, $\mathcal{B}(B \to e\nu) << \mathcal{B}(B \to \mu\nu) << \mathcal{B}(B \to \tau\nu)$. $B \to e\nu$ and $B \to \mu\nu$ decay modes are out of reach at current B-factories unlike $B \to \tau\nu$. This mode is also a probe for physics beyond the SM. In particular it can be mediated at tree level by a charged Higgs boson and consequently its branching ratio would be modified with this additional contribution.

In the analysis of $B^+ \to \tau^+\nu_\tau$ decays, the τ^+ lepton is reconstructed in four decay modes which represent

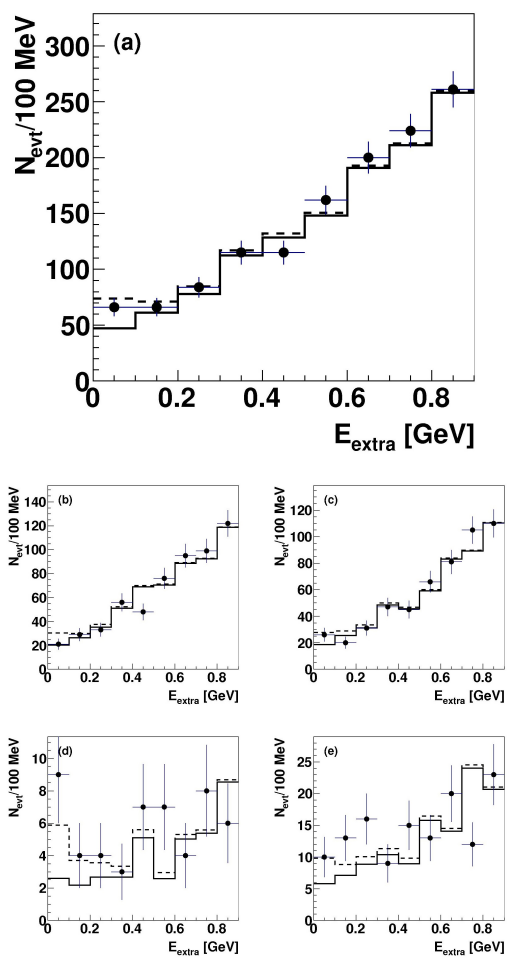

Figure 1: Distribution of $E_{\rm extra}$ in data (points with error bars) with the results of the simultaneous fit on the four analyzed τ decay modes overlaid. The solid line shows the contribution of the background only, while the dashed line shows the total fit result. The top plot (a) shows all τ decay modes combined, while the lower plots show each mode individually: (b) $e^+\nu_e\bar{\nu}_\tau$, (c) $\mu^+\nu_\mu\bar{\nu}_\tau$, (d) $\pi^+\bar{\nu}_\tau$, and (e) $\rho^+\bar{\nu}_\tau$.

about 70% of the total decay width: $e^+\nu_e\bar{\nu}_\tau$, $\mu^+\nu_\mu\bar{\nu}_\tau$, $\pi^+\bar{\nu}_\tau$, and $\rho^+\bar{\nu}_\tau$ with $\rho^+ \to \pi^+\pi^0$. As these four modes contain only one charged particle in the final state, the analysis requires that there is only one reconstructed track on the signal side. In addition for signal events there should be small residual energy in the calorimeter, so the best discriminating variable is this residual energy, $E_{\rm extra}$, defined as the sum of the energy of all clusters detected in the electromagnetic calorimeter above a threshold of 60 MeV after removing those associated to the fully reconstructed tag-B meson and the τ lepton decay products. The $B \to \tau\nu$ branching fraction is obtained from a maximum likelihood fit to $E_{\rm extra}$, performed simultaneously in the four τ decay sub-modes considered. The shape for $E_{\rm extra}$ is obtained from tag-B-mass sideband in data for the combinatorial background, and Monte Carlo (MC) for the signal and peaking background. Double tagged events, where the two B mesons are fully reconstructed, are used to validate the MC.

Figure 1 illustrates the results of the fit separately for the four sub-modes and also for the sum of all sub-modes. With 62 ± 17 signal events, seen at small values of $E_{\rm extra}$, the following branching ratio is measured (where two uncertainties are given, the first is statistical and the second is systematic):

$\mathcal{B}(B^+ \to \tau^+\nu_\tau) = (1.83^{+0.53}_{-0.49} \pm 0.24) \times 10^{-4}$.

The dominant systematic error comes from modeling the background probability density functions. Taking into account the systematic uncertainty, the significance of the branching ratio measurement is 3.8 σ.

Table 1: Published results for the $B \to \tau\nu$ branching ratio from *BABAR* and Belle collaborations.

Experiment	Tag	$\mathcal{B}(B \to \tau\nu)$ ($\times 10^{-4}$)
BABAR	hadronic [4]	$1.8^{+0.9}_{-0.8} \pm 0.4 \pm 0.2$
BABAR	semileptonic [5]	$1.7 \pm 0.8 \pm 0.2$
Belle	hadronic [6]	$1.79^{+0.56+0.46}_{-0.49-0.51}$
Belle	semileptonic [7]	$1.54^{+0.38+0.29}_{-0.37-0.31}$

This new result is compatible with previous measurements from *BABAR* and Belle using either hadronic or semileptonic tags [4, 5, 6, 7], shown in Table 1. When we now compare our result with the SM prediction, $\mathcal{B}_{SM}(B \to \tau\nu) = 0.62 \pm 0.12$ if calculating it with the exclusive measurement of $|V_{ub}|$ by *BABAR* [8], or $\mathcal{B}_{SM}(B \to \tau\nu) = 1.18 \pm 0.16$ if using the inclusive measurement [9], and in both cases the lattice QCD calculation of $f_B = 189 \pm 4$ MeV [10], we find an excess of 2.4 σ in the former case and 1.6 σ in the latter case. However, Belle recently presented a new result [11], also with hadronic tags, $\mathcal{B}(B^+ \to \tau^+\nu_\tau) = (0.72^{+0.27}_{-0.25} \pm 0.11) \times 10^{-4}$, which is somewhat lower, though still compatible with our result.

The $B \to \tau\nu$ branching ratio measurement can be used to constraint models beyond the SM, especially those involving a charged Higgs boson. In this context, the most commonly used model is the type-II two-Higgs-doublet model (2HDM). The $B \to \tau\nu$ branching fraction is predicted in this model [12], as a function of the ratio $\tan\beta/m_{H^+}$, where $\tan\beta$ is the ratio of the vacuum expectation values between the two Higgs doublets and m_{H^+} the charged Higgs mass:

$$\frac{\mathcal{B}_{2HDM}(B^+\to\ell^+\nu)}{\mathcal{B}_{SM}(B^+\to\ell^+\nu)} = \left(1 - \tan^2\beta\frac{m_B^2}{m_{H^+}^2}\right)^2.$$

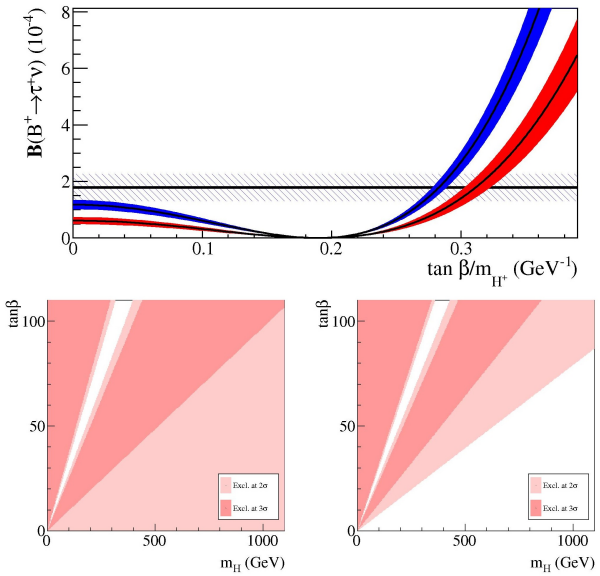

Figure 2: Top plot: Comparison between the measured $B \to \tau\nu$ branching ratio (horizontal band) with the prediction of the 2HDM as a function of $\tan\beta/m_{H^+}$ using the exlusive (red/light gray) or inclusive (blue/dark gray) $|V_{ub}|$ measurement. Bottom plots: 2 and 3 σ exclusion regions in the $m_{H^+} - \tan\beta$ plane using the (left) exlusive or (right) inclusive $|V_{ub}|$ measurement.

Figure 2 compares our measured $B \to \tau\nu$ branching ratio with the prediction of the 2HDM using either the exlusive or inclusive $|V_{ub}|$ measurement as a function of $\tan\beta/m_{H^+}$. Most values of the ratio $\tan\beta/m_{H^+}$ can be exluded, except a value of about 0.3 and also small values of this ratio especially when using the inclusive $|V_{ub}|$ measurement. In fact, almost all of the parameter plane $m_{H^+} - \tan\beta$ is excluded at 95% confidence level when assuming the $|V_{ub}|$ exclusive determination. Using $|V_{ub}|$ inclusive measurement, the constraints are less stringent, but nethertheless Higgs masses up to 1 TeV can be excluded at 95% confidence level for $\tan\beta$ greater than 70.

3. $B \to D^{(*)}\tau\nu$ decays

The measurement of the semileptonic decay $B \to D^{(*)}\ell\nu$ allows to test the SM, whose prediction of its differential decay rate as a function of the square of the mass of the virtual W, q^2, is:

$$\frac{d\Gamma}{dq^2} = \frac{G_F^2|V_{cb}|^2 |p_{D^{(*)}}| q^2}{96\pi^3 m_B^2}\left(1 - \frac{m_\ell^2}{q^2}\right)^2 \left[(|H_+|^2 + |H_-|^2 + |H_0|^2)(1 + \frac{m_\ell^2}{2q^2}) + \frac{3m_\ell^2}{2q^2}|H_s|^2\right].$$

$p_{D^{(*)}}$ is the momentum of the $D^{(*)}$ in the B rest frame. H_+, H_-, H_0, and H_s are the hadronic currents for the three vector states and the scalar state. The former two contribute only to the $B \to D^*\ell\nu$ channel.

As in the previous analysis, constraints can be put on models beyond the SM, since here also a charged Higgs boson can contribute to the decay at tree level. As the Higgs boson is spinless, its contribution would enter the decay rate in the scalar hadronic amplitude H_s, which is weighted by the square of the lepton mass and therefore would be seen mainly in the τ channel.

The analysis will determine the two ratios $R(D) = \frac{\mathcal{B}(\bar{B}\to D\tau^-\bar{\nu}_\tau)}{\mathcal{B}(\bar{B}\to D\ell^-\bar{\nu}_\ell)}$ and $R(D^*) = \frac{\mathcal{B}(\bar{B}\to D^*\tau^-\bar{\nu}_\tau)}{\mathcal{B}(\bar{B}\to D^*\ell^-\bar{\nu}_\ell)}$, where ℓ is either an electron or a muon. Doing this cancels several sources of experimental (for example reconstruction efficiencies) and theoretical (for example $|V_{cb}|$) uncertainties.

A lot of efforts have been put the improve the tagging efficiency. The tag-B is reconstructed in a charmed meson and several charged or neutral pions and kaons. With respect to the previous analysis [13], the number of decay chains has increased from 630 to 1768, increasing the efficiency by a factor two up to 0.4%, at the price of a somewhat degraded purity, as illustrated in Figure 3.

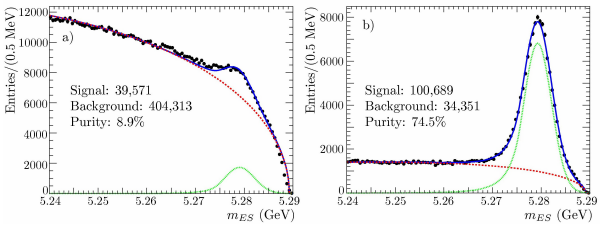

Figure 3: Distributions of the tag-B reconstructed mass in a) a 5 fb^{-1} data sample and b) a MC simulation. The green dotted curve shows the signal, the red dashed curve the background, and the blue solid curve the sum of the two.

Taus are reconstructed in their purely leptonic decays, $e\nu\bar{\nu}$ or $\mu\nu\bar{\nu}$, so that the $B \to D^{(*)}\tau\nu$ signal and $B \to D^{(*)}\ell\nu$ normalization modes have exactly the same reconstructed particles. They differ only by the number of neutrinos. The yields are extracted by an unbinned maximum likelihood fit using two variables: the electron or muon momentum in the B rest frame, p_l^*, and the square of the missing mass, $m^2_{\rm miss}$, which is peaked at zero for the normalization channels where there is only one neutrino, but has a broad distribution for the signal channels with three neutrinos. The following yields are left free to vary in the fit for each of the four channels with D^0, D^+, D^{*0}, and D^{*+}: the $B \to D^{(*)}\tau\nu$ signal, the $B \to D^{(*)}\ell\nu$ normalization and the $D^{**}l\nu$ background, which is the most troublesome background, while com-

binatorial and continuum background yields are fixed at values obtained with control samples.

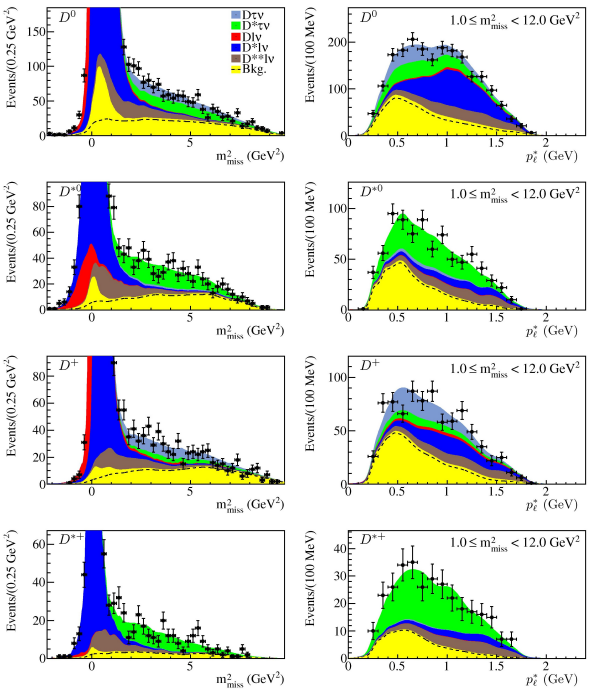

Figure 4: Projections of the fit to the signal sample in (left) $m^2_{\rm miss}$ and (right) p^*_l for (top to bottom) the D^0, D^{*0}, D^+, and D^{*+} channels. The p^*_l projections do not include the region $m^2_{\rm miss} < 1$ GeV^2, where the normalization channels (dark blue/dark gray) peak.

Figure 4 shows the fit results in the four $B \to D^{(*)}\tau\nu$ channels, with neutral and charged D and D^*. The peak at zero in the missing mass square distributions can be clearly seen for the normalization channels $B \to D^{(*)}\ell\nu$, while the $B \to D^{(*)}\tau\nu$ signals are found at higher values of $m^2_{\rm miss}$. The cross-feed from $D\tau\nu$ to $D^*\tau\nu$ is small, while there is a significant cross-feed from $D^*\tau\nu$ to $D\tau\nu$. Respectively 639 ± 62 and 245 ± 27 signal events are observed in the $D^{*0}\tau\nu$ and $D^{*+}\tau\nu$ channels with a statistical significance greater than 11 σ. Similarly 314 ± 60 and 177 ± 31 signal events are found in the $D^0\tau\nu$ and $D^+\tau\nu$ channels respectively, leading to a first observation with more than 5 σ statistical significance in these channels. The charged and neutral channels give compatible results and are combined in an isospin-constrained fit to get the final results.

The systematic uncertainty in the measurements of R(D) and R(D*) is dominated by the background contribution, and in particular the $B \to D^{**}\ell\nu$ background. Control samples, such as $D^{(*)}\pi^0 l\nu$, are used to check that the shape of this background in missing mass square and lepton momentum is well described. In contrast, the uncertainty coming from the ratio of efficiencies in the signal and normalization channels is not a dominant source of uncertainty. Overall the statistic uncertainty is greater than the systematic uncertainty.

The results are shown in Table 2. $B \to D\tau\nu$ is observed for the first time with more than 5 σ significance with a branching fraction of $(1.02 \pm 0.13 \pm 0.11)\%$, while the branching fraction measured for $B \to D^*\tau\nu$ is $(1.76 \pm 0.13 \pm 0.12)\%$. The $R(D)$ and $R(D^*)$ branching fraction ratios are determined to be respectively $0.440 \pm 0.058 \pm 0.042$ and $0.332 \pm 0.024 \pm 0.018$. They are compatible with previous measurements from *BABAR* [13] and Belle [14, 15, 16] and more precise. All measurements have always been higher than the SM prediction.

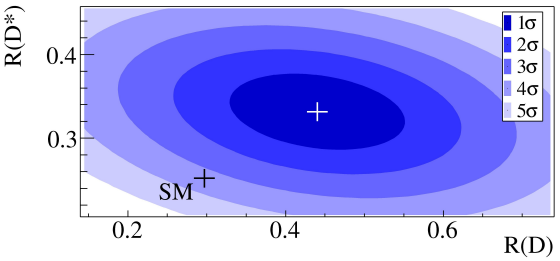

Figure 5: Comparison in the $R(D)$ - $R(D^*)$ plane between the measurement (white cross) and the SM prediction (black cross).

Figure 5 compares the new results with the SM prediction: $R_{SM}(D) = 0.297 \pm 0.017$ and $R_{SM}(D^*) = 0.252 \pm 0.003$. The measured values of R(D) and R(D*) are respectively 2.0 σ and 2.7 σ above the prediction. When combining the two results, taking into account their -27% correlation, the SM prediction is 3.4 σ away from the measurement.

Can a charged Higgs explain the discrepancy? As in the previous analysis, the measurements are used to check the type-II two-Higgs-doublet model. In this model, the scalar hadronic current is modified according to the following expression [17] (where the $-$ sign is for $D\tau\nu$ and the $+$ sign for $D^*\tau\nu$):

$$\frac{H_s^{2HDM}}{H_s^{SM}} \sim \left(1 - \frac{\tan^2\beta}{m^2_{H^+}} \frac{q^2}{1 \mp m_c/m_b}\right).$$

Figure 6 shows the value of $\tan\beta/m_{H^+}$ for which the prediction in the 2HDM model matches the measurement. The values of $\tan\beta/m_{H^+}$ found in this way, 0.44 ± 0.02 for $R(D)$ and 0.75 ± 0.04 for $R(D^*)$, cannot be accomodated at the same time. So the 2HDM is excluded in the full parameter space with a probability greater than 99.8%.

Table 2: Results of the isospin-unconstrained (top four rows) and isospin-constrained fits (last two rows). The columns show the signal and normalization yields, $R(D^{(*)})$, branching fractions, and $\Sigma_{\rm stat}$ and $\Sigma_{\rm tot}$, the statistical and total significances. The branching fractions $\mathcal{B}(B \to D^{(*)}\tau\nu)$ are calculated as $R(D^{(*)}) \times \mathcal{B}(B \to D^{(*)}\ell\nu)$, using the average $B \to D^{(*)}\ell\nu$ branching fractions measured by *BABAR*.

Decay		$N_{\rm sig}$	$N_{\rm norm}$	$R(D^{(*)})$	$\mathcal{B}(B \to D^{(*)}\tau\nu)\,(\%)$	$\Sigma_{\rm stat}$	$\Sigma_{\rm tot}$
$B^- \to$	$D^0\tau^-\bar{\nu}_\tau$	314 ± 60	1995 ± 55	$0.429 \pm 0.082 \pm 0.052$	$0.99 \pm 0.19 \pm 0.13$	5.5	4.7
$B^- \to$	$D^{*0}\tau^-\bar{\nu}_\tau$	639 ± 62	8766 ± 104	$0.322 \pm 0.032 \pm 0.022$	$1.71 \pm 0.17 \pm 0.13$	11.3	9.4
$\bar{B}^0 \to$	$D^+\tau^-\bar{\nu}_\tau$	177 ± 31	986 ± 35	$0.469 \pm 0.084 \pm 0.053$	$1.01 \pm 0.18 \pm 0.12$	6.1	5.2
$\bar{B}^0 \to$	$D^{*+}\tau^-\bar{\nu}_\tau$	245 ± 27	3186 ± 61	$0.355 \pm 0.039 \pm 0.021$	$1.74 \pm 0.19 \pm 0.12$	11.6	10.4
$\bar{B} \to$	$D\tau^-\bar{\nu}_\tau$	489 ± 63	2981 ± 65	$0.440 \pm 0.058 \pm 0.042$	$1.02 \pm 0.13 \pm 0.11$	8.4	6.8
$\bar{B} \to$	$D^*\tau^-\bar{\nu}_\tau$	888 ± 63	11953 ± 122	$0.332 \pm 0.024 \pm 0.018$	$1.76 \pm 0.13 \pm 0.12$	16.4	13.2

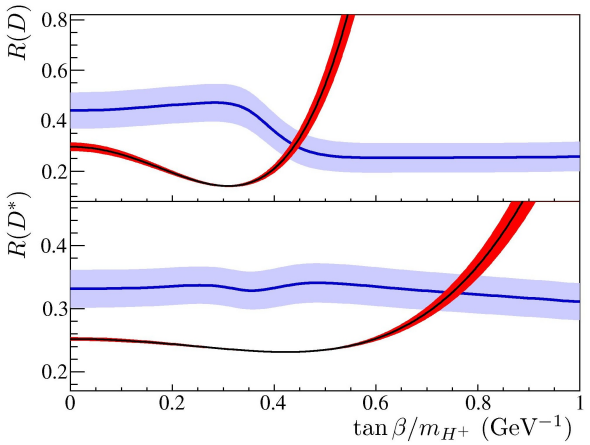

Figure 6: Comparison between the measured (top) $R(D)$ and (bottom) $R(D^*)$ (blue/light gray) with the prediction of the 2HDM (red/dark gray) as a function of $\tan\beta/m_{H^+}$.

4. Conclusion

In summary, *BABAR* has updated its measurement of $\mathcal{B}(B^+ \to \tau^+\nu_\tau) = 1.83^{+0.53}_{-0.49} \pm 0.24$, which, unlike the new result from Belle, is about 2 σ above the SM prediction.

Besides, an improved measurement of the ratios of $B \to D^{(*)}\tau\nu$ over $B \to D^{(*)}\ell\nu$ branching fractions has been obtained by *BABAR*: $R(D) = 0.440 \pm 0.058 \pm 0.042$ and $R(D^*) = 0.332 \pm 0.024 \pm 0.018$. These results, when combined, disagree with the SM at the 3.4 σ level and show evidence for an excess with respect to the SM expectations. However, the results cannot be explained by the 2HDM for any value of its parameters.

References

[1] J. Lees, et al., Evidence of $B \to \tau\nu$ decays with hadronic B tags, submitted to Phys.Rev. D. arXiv:1207.0698.

[2] J. Lees, et al., Evidence for an excess of $\bar{B} \to D^{(*)}\tau^-\bar{\nu}_\tau$ decays, Phys.Rev.Lett. 109 (2012) 101802. arXiv:1205.5442, doi:10.1103/PhysRevLett.109.101802.

[3] B. Aubert, et al., The BaBar detector, Nucl.Instrum.Meth. A479 (2002) 1–116. arXiv:hep-ex/0105044, doi:10.1016/S0168-9002(01)02012-5.

[4] B. Aubert, et al., A Search for $B^+ \to \tau^+\nu$ with Hadronic B tags, Phys.Rev. D77 (2008) 011107. arXiv:0708.2260, doi:10.1103/PhysRevD.77.011107.

[5] B. Aubert, et al., A Search for $B^+ \to \ell^+\nu_\ell$ Recoiling Against $B^- \to D^0\ell^-\bar{\nu}X$, Phys.Rev. D81 (2010) 051101. arXiv:0912.2453, doi:10.1103/PhysRevD.81.051101.

[6] K. Ikado, et al., Evidence of the Purely Leptonic Decay $B^- \to \tau^-\bar{\nu}_\tau$, Phys.Rev.Lett. 97 (2006) 251802. arXiv:hep-ex/0604018, doi:10.1103/PhysRevLett.97.251802.

[7] K. Hara, et al., Evidence for $B^- \to \tau^-\bar{\nu}$ with a Semileptonic Tagging Method, Phys.Rev. D82 (2010) 071101. arXiv:1006.4201, doi:10.1103/PhysRevD.82.071101.

[8] M. F. Sevilla, Measurements of $\bar{B} \to D^{(*)}\tau^-\bar{\nu}_\tau$ and $|V_{ub}|$ at BaBar, PoS EPS-HEP2011 (2011) 155.

[9] J. Lees, et al., Study of $\bar{B} \to X_u\ell\bar{\nu}$ decays in $B\bar{B}$ events tagged by a fully reconstructed B-meson decay and determination of $|V_{ub}|$, Phys.Rev. D86 (2012) 032004. arXiv:1112.0702, doi:10.1103/PhysRevD.86.032004.

[10] H. Na, C. J. Monahan, C. T. Davies, R. Horgan, G. P. Lepage, et al., The B and B_s Meson Decay Constants from Lattice QCD, Phys.Rev. D86 (2012) 034506. arXiv:1202.4914, doi:10.1103/PhysRevD.86.034506.

[11] I. Adachi, et al., Measurement of $B^- \to \tau^-\bar{\nu}_\tau$ with a Hadronic Tagging Method Using the Full Data Sample of Belle, arXiv:1208.4678.

[12] W.-S. Hou, Enhanced charged Higgs boson effects in $B^- \to \tau\bar{\nu}, \mu\bar{\nu}$ and $b \to \tau\bar{\nu} + X$, Phys.Rev. D48 (1993) 2342–2344. doi:10.1103/PhysRevD.48.2342.

[13] B. Aubert, et al., Observation of the semileptonic decays $B \to D^*\tau^-\bar{\nu}_\tau$ and evidence for $B \to D\tau^-\bar{\nu}_\tau$, Phys.Rev.Lett. 100 (2008) 021801. arXiv:0709.1698, doi:10.1103/PhysRevLett.100.021801.

[14] A. Matyja, et al., Observation of $B^0 \to D^{*-}\tau^+\nu_\tau$ decay at Belle, Phys.Rev.Lett. 99 (2007) 191807. arXiv:0706.4429, doi:10.1103/PhysRevLett.99.191807.

[15] I. Adachi, et al., Measurement of $B \to D^{(*)}\tau\nu$ using full reconstruction tags, arXiv:0910.4301.

[16] A. Bozek, et al., Observation of $B^+ \to \bar{D}^{*0}\tau^+\nu_\tau$ and Evidence for $B^+ \to \bar{D}^0\tau^+\nu_\tau$ at Belle, Phys.Rev. D82 (2010) 072005. arXiv:1005.2302, doi:10.1103/PhysRevD.82.072005.

[17] M. Tanaka, R. Watanabe, Tau longitudinal polarization in $B \to D\tau\nu$ and its role in the search for charged Higgs boson, Phys.Rev. D82 (2010) 034027. arXiv:1005.4306, doi:10.1103/PhysRevD.82.034027.